ESJ Natural/Life/Medical Sciences Peer-reviewed

Structural Evolution and its Implication for the Emplacement of Gold Deposit in the Central Part of Burkina Faso, West Africa

Ernest Gomdebziige Ouedraogo
Nicolas Kagambega
Université de Fada N'Gourma/Département Génie Minier, Burkina Faso
Laboratoire Geosciences et Environnement, Ouagadougou, Burkina Faso
Saga Sawadogo
Université Joseph Ki ZERBO/Laboratoire Geosciences et Environnement, Ouagadougou, Burkina Faso
Hubert G. Zongo
Madi Ouedraogo
Université de Fada N'Gourma/Département Génie Minier, Burkina Faso
Laboratoire Geosciences et Environnement, Ouagadougou, Burkina Faso
Martin Lompo
Université Joseph Ki ZERBO/Laboratoire Geosciences et Environnement, Ouagadougou, Burkina Faso

Doi:10.19044/esj.2024.v20n3p213

Submitted: 29 December 2023
Accepted: 29 January 2024
Published: 31 January 2024

Cite As:
Ouedraogo G.E., Kagambega N., Sawadogo S., Zongo H.G., Ouedraogo M. & Lompo M. (2024). *Structural Evolution and its Implication for the Emplacement of Gold Deposit in the Central Part of Burkina Faso, West Africa.* European Scientific Journal, ESJ, 20 (3), 213. https://doi.org/10.19044/esj.2024.v20n3p213

Abstract

In order to constrain the structural evolution in the central part of Burkina Faso and its implication for the emplacement of gold deposits, we undertook a structural mapping by coupling Landsat and aeromagnetic images interpretation to outcrop and core mapping followed by laboratory work. This approach reveals that the structural architecture in this locality mainly results from dextral transcurrent progressive deformation due to a NW-SE trending major stress. This architecture is similar to the Riedel-Tchalenko model. Initially, the dominant normal stress created an E-W constriction resulting in the development of N-S shear corridors. Subsequently, the tangential stress

 ISSN: 1857-7881 (Print) e - ISSN 1857-7431

that took over this generated the progressive development of simple dextral shear zones with a NE-SW orientation that are locally taken up by ENE-WSW dextral shear bands associated with the Riedel's R structures. As a result of the cooling of the crust, we are witnessing the formation of sinistral NW-SE and dextral NNE-SSW strike-slip faults, respectively, which corresponds to Riedel's R' structures and Tchalenko's P structures. The development of NW-SE pre-Eburnean shear zones, particularly the N-S shear corridors, is synchronous with the circulation of gold-bearing fluids through the zone. However, the intersections of these directional corridors create zones suitable for gold concentration. Within these zones, ductile-brittle deformation following the emplacement of the shear bands has facilitated the remobilization and concentration of gold-bearing fluids within rocks with the appropriate rheological conditions. This is the case for Toega gold deposit.

Keywords: Structural, Riedel system, Nakomgo, Toega

Introduction

Most of the gold deposits in the Paleoproterozoic basement of Burkina Faso, like those described throughout the West African craton, are classified as orogenic gold type (Mélisi *et al.*, 1992; Béziat *et al.*, 2008; Markwitz *et al.*, 2015; David *et al.*, 2018). At any scales, the spatial distribution of gold is largely controlled by structural deformation (Lompo, 2010; David *et al.*, 2018). On a regional scale, most deposits and bodies discovered on the Paleoproterozoic basement are located along NE-SW transcurrent shear corridors and associated relay structures (Feybesse *et al.*, 2006; Dubé & Gosselin, 2007; Murray *et al.*, 2019). At the district or deposit scale, mineralization is associated with a variety of faults and shear zones formed prior to the mineral episode but remains fully confined between subparallel relay fracture pairs intersecting early structures. Gold concentrations are thought to be developed in dilation zones created within blocks exposed by early structures (David *et al.*, 2018). Sometimes, the deposits are carried by folds, particularly at their anticlinals (Tunks *et al.*, 2004). In any cases, orogenic gold commonly occurs in bedding, lithological contacts, parallel shear zones, stockwork veins, and in quartz veins related to brittle-ductile shear zones (Baratoux *et al.*, 2015; Markwitz *et al.*, 2016). Therefore, detail study of structural deformation evolution within a locality may be a good tool to mineral resource surveying and modeling. However, while most authors agree on the structural control of gold mineralization within the Leo Ridge and Burkina Faso, this is not the case for the structural evolution at both the regional and local scales.

Indeed, several studies undertaken at the scale of the Leo Ridge and at the local scale have often led to different results and sometimes conflicting.

 ISSN: 1857-7881 (Print) e - ISSN 1857-7431

For example, on a regional scale, the main shear corridors indicate some ramifications leading to secondary relay structures. Also, it was interpreted as the result of a progressive deformation initiated with vertical tectonics synchronous to a diapiric ascension of the magma, which is followed by a transcurrent tectonics (Vidal *et al.*, 2009; Lompo, 2010). In contrast, other authors have described an anastomosed transpressional network resulting from the three-dimensional partitioning of progressive transpressional deformation. This network involves interactions among shear zones that absorb heterogeneities in the regional flow patterns while maintaining the connectivity of the shear zone network (Chardon *et al.*, 2020). These interpretations are significantly different from that proposed by most authors who attempt to organize the different deformation structures observed into tectonic phases. Thus, in several localities of Burkina Faso, including the central part as well as everywhere else across the ridge, different tectonic phases sometimes conflicting have been described (Allibone *et al.*, 2002; Hein, 2004; Feybesse *et al.*, 2006, Tshibubudze *et al.*, 2009; 2013; 2015; Ouiya *et al.*, 2015; Fontaine *et al.*, 2017; Sawadogo *et al.*, 2018; Siagné *et al.*, 2022), extending the debate on the structural evolution of the Paleotroterozoic basement.

This paper focuses on describing the structural evolution in the central part of Burkina Faso by proposing a structural model and its implication in mineralization. Additionally, this research provides more details on the deformation structures in this part of the country. To achieve this, Landsat 8 and aeromagnetic data will be coupled with lithostructural mapping on outcrops and cores. These different data will be subsequently improved through the description and measurement of microstructures that constitute key markers of the kinematics of the deformation.

Geological Setting

The study area covers the south-central part of Burkina Faso. It is a vast open forest peneplain with lateritic mounds and some hill outcrops as its main positive features. Geologically, the study area (Figure 1a) is located in the northeastern part of Baoule-Mossi domain composed of formations of Paleoproterozoic age and forming part of Paleoproterozoic basement. This domain, along with the Kénéma-Man domain, comprises the Leo Ridge. This is located in the southern part of West African Craton and separated from Reguibat ridge in the north by the Taoudéni sedimentary basin. These two entities, ridge and basin, are bounded to the east and west by Hercynian and Pan-African mobile chains (Boher *et al.*, 1992; Ferré & Caby, 2007).

The general composition of Paleoproterozoic basement of Baoulé-Mossi domain shows more or less deformed and weakly metamorphosed plutono-volcanic and sedimentary formations in the regional greenschist

 ISSN: 1857-7881 (Print) e - ISSN 1857-7431

facies commonly called greenstone belts. These belts are generally NE-SW trending (Allibone *et al.*, 2002; Soumaila *et al.*, 2004; Feybesse *et al.*, 2006; Lompo, 2009; Baratoux *et al.*, 2011; Augustin *et al.*, 2017). They are separated by large batholiths of granitoid at the contact of which zones marked by high-grade contact metamorphism are sometimes noted. These formations are locally cut by dolerite veins indicating WNW-ESE, ENE-WSW, and NE-SW orientation (Wenmenga *et al.*, 2009; Metelka *et al.*, 2011).

Locally, the zone is located within the southwestern Liptako-Fada N'Gourma province (Ducellier, 1963; Hottin & Ouédraogo, 1975) and incorporates a portion of the Tiébélé-Dori-Markoye Fault (Tshibubudze *et al.*, 2012; Chardon *et al.*, 2020). As shown in Figure 1b, it comprises of a polydeformed and metamorphosed volcano-sedimentary unit forming the NE-SW trending belts, intercalated by banded Tonalite-Trondhjemite-Granodiorite plutonic formations, weakly foliated plutons and sometimes undeformed alkaline intrusive rocks (Pons *et al.*, 1995; Castaing *et al.*, 2003; Kagambèga *et al.*, 2004; Naba *et al.*, 2004). At Nakomgo permit scale, the intrusive rocks are represented by biotite and often amphibole granites showing variable structures. In addition, tonalites, granodiorites, quartz diorites, gabbros, and dolerites are present, as well as amphibolites. The sedimentary deposits are composed of conglomerates and sandstones showing variable grain sizes. These two units are more or less deformed and metamorphosed into a green schist facies, particularly amphibolites, and locally exhibit migmatitic facies at the contacts of plutons. They are intercalated by volcano-sedimentary schists. This complex is intersected by dolerite dykes trending NW-SE. The common characteristics to all these formations are silicification marked by the presence of veins and sub-grains of quartz, as well as the carbonation linked to the recurrent presence of calcite veinlets or disseminated crystals.

Tectonically, the structural deformation is mainly marked in the region by the Tiébélé-Dori-Markoye fault (Tshibubudze *et al.*, 2009). This is a shear corridor of more than 400 km crossing the country from north to south in a general NNE-SSW direction and is estimated to be 5 km wide in the vicinity of Markoye. This mega deformation corridor is punctuated by subsidiary corridors with a general NE-SW orientation such as the Bol-Bolgatenga shear corridor in the south (Woodman *et al.*, 2015), the Bomboré and Zam shear corridors (Castaing *et al.*, 2003) in the vicinity of Mogteodo in the center, and the Saogo, Mukossi and Billiata mylonitic zones in the north (Tshibubudze *et al.*, 2009). Some NW-SE corridors are also reported. These include the Essakane thrust zones and the Dori and Sokadié shear zones in the north

 ISSN: 1857-7881 (Print) e - ISSN 1857-7431

(Tshibubudze *et al.*, 2009; 2013; 2015), and the NNW-SSE Tanlouka shear zones in the center (Sawadogo *et al.*, 2021).

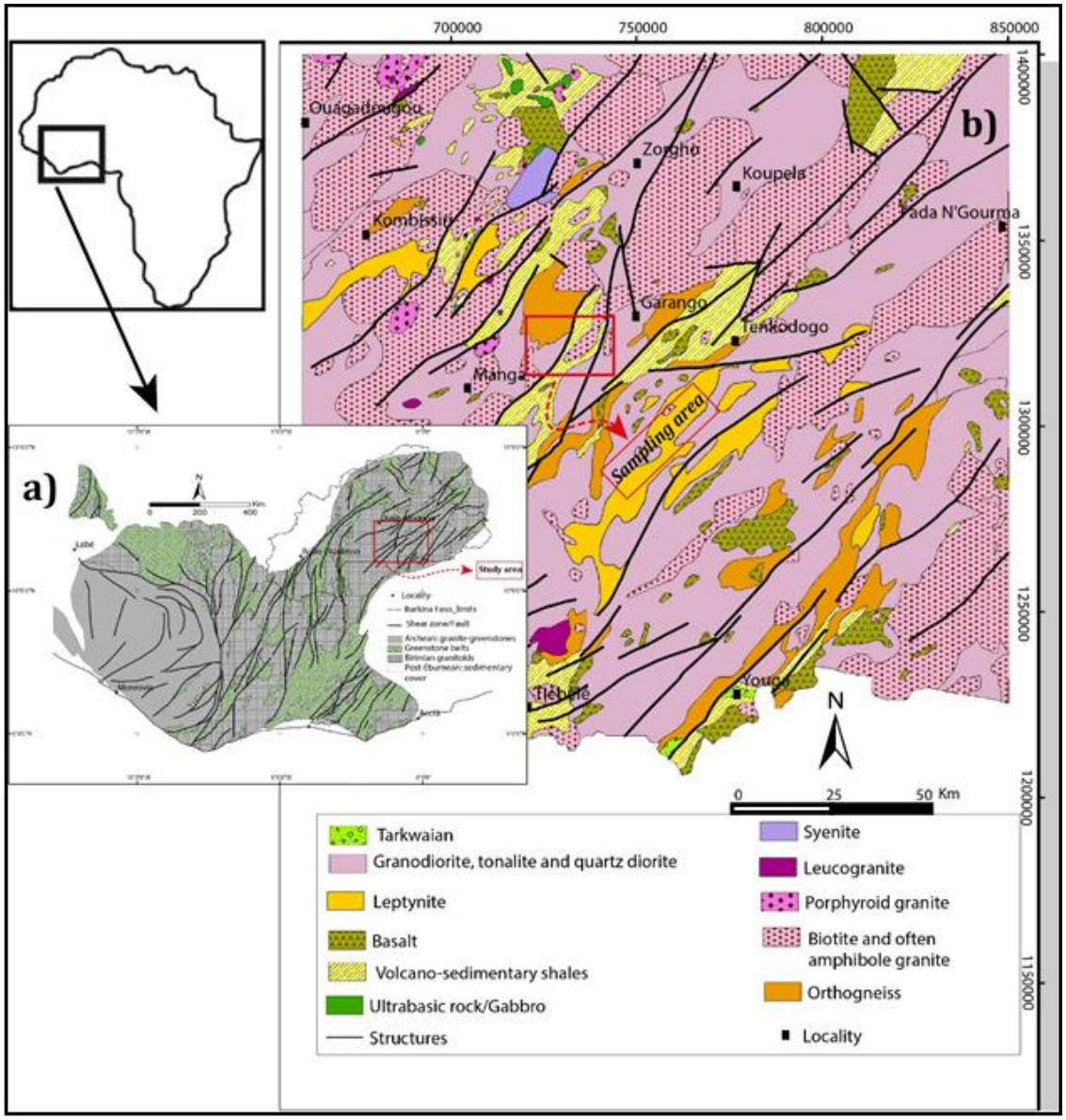

Figure 1. a) Structural map of the southern West Africa craton (modified after Chardon et al., 2020); **b)** Geological map of the study area (modified after Castaing et al., 2003). The sampling area represents the Nakomgo permit.

Methodology

Four approaches were combined to obtain the expected results. These are: (i) Landsat 8 and aeromagnetic image interpretation, (ii) outcrop and core mapping, (iii) microscopy, and (iv) geochemistry through ICP-MS.

 ISSN: 1857-7881 (Print) e - ISSN 1857-7431

Landsat 8 and Aeromagnetic Images

The interpretation of Landsat and aeromagnetic images is very important to initiate a structural study in a locality. By plotting lineaments on a large scale, it gives an overview of the area and allows the targeting of different areas of interest for field mapping. The Landsat 8 image used was downloaded from the U.S. Geological Survey (USGS) website on February 25, 2020 via the Global Mapper 19 application. We made corrections tending to further expose the various lineaments and lithologic contacts (Figure 2a). The aeromagnetic images we received from West African Resources are from BUMIGEB ("*Bureau des Mines et de la Géologie du Burkina*"). They have also undergone several treatments tending to express the different lineaments and lithological contacts (Figure 2b).

Outcrop and Core mapping

Field work is consisted of observations, structural measurements, and sampling at both surface and depth. The depth rocks were accessed via oriented core from the diamond drill holes. Macroscopic observations were made to characterize the petrography, identify and describe the deformation structures, and establish their spatial and temporal relationships. They also allowed the identification of sampling zones for laboratory studies. The structural measurements were carried out by using a compass with a clinometer. Rocks subjected to physical constraints different from those which prevailed at their setting can be deformed by distortion or by rupture. This often results in planar and linear structures characterized by orientation, dip, and dip-direction (Ramsay, 1967). In summary, various planar structures have been identified on outcrops and measured by application of the right-hand rule. Some of them contain linear structures, notably stretching and mineral lineations on foliation planes, as well as striations on fault mirrors. We also measured these linear structures. Concerning the structures identified on the cores, we were able to measure the geometry of the planar features with a goniometer using the alpha, beta, and gamma method. These data were then converted to dip and dip-direction using Excel tables.

In terms of sampling, three criteria guided the choice of adequate sampling area (Passchier & Rudolph, 2005). These include:

1. **The Lithological Criterion:** Very fine-grained formations were particularly sampled because of their ability to memorize deformation.
2. **The Presence of Pebbles or Porphyroclasts:** The study of their geometry can define, in some contexts, the mechanism of deformation.
3. **The Superimposition Relationships of Structures:** They allow for the constraint of the chronology of tectonic events.

 ISSN: 1857-7881 (Print) e - ISSN 1857-7431

In particular, the rock core sampling concerned mainly the mineralized zones and their immediate surroundings as well as waste rocks. These so-called barren and mineralized zones were determined using gold content data obtained by ICP-MS analysis. This method is presented in detail below. To facilitate the structural analysis, we grouped the structural data into ductile deformation structures represented by schistosity/foliation and lineation, brittle-ductile and brittle structures represented by veins, fractures, and faults. Then, we proceeded to the stereographic projection of all these structures separately using the GEOrient 9.5 software.

Microscopic Analysis

The microscopic analysis was limited to descriptions and measurements of microstructures on oriented thin sections in order to further constrain the petrography and especially the deformation. It was carried out in the laboratory for thin sectioning and microscopy of the University of Fada N'Gourma in Burkina Faso. The preparation of oriented thin sections was done on the basis of oriented samples collected in the field and on the cores. Each sample was cut into three specimens along the main planes of deformation (X, Z), (X, Y), and (Y, Z). This is because under the effect of flattening or shearing, a volume of material responds to mechanical stresses by developing:

- a (X, Y) plane of flattening or shearing corresponding to the plane of foliation perpendicular to the main direction of shortening Z;
- a plane (Y, Z) perpendicular to the axis of the greatest elongation X and
- a plane (X, Z) parallel to the lineation and perpendicular to the axis of the smallest elongation Y.

When this volume of material contains geological objects such as porphyroclasts, they will change shape along the three axes (X, Y, Z). The use of geometric features of the deformed object observable in the (X, Z) and (Y, Z) planes allows to better constrain the kinematic analysis (Passchier & Rudolph, 2005).

ICP-MS Analysis

The acquisition of gold assay data from the reverse circulation (RC) and diamond drilling (DD) boreholes was made possible by the ICP-MS method (inductively coupled plasma mass spectrometry) used by the ALS analysis laboratory through its subsidiary based in Ouagadougou, Burkina Faso. Drilling was carried out on a 60 x 60 meters grid with an azimuth of 270° and an inclination of -65°. Sampling, generally done per meter of drilling, took into account the lithology and deformation.

 ISSN: 1857-7881 (Print) e - ISSN 1857-7431

Results

Lineaments

Interpretation of Landsat 8 and aeromagnetic images has allowed us to identify three major deformation corridors separated on either side by the granitoids. These corridors appear as a network of relatively small bands and generally have a NE-SW orientation, as shown by the rose diagram on the lineament map (Figure 2). However, their trajectory is sinuous in detail. These three deformation corridors are associated with more or less isolated lineaments of various orientations, sometimes intersecting all the structures. Concentric structures are locally observed.

Structures of the Deformation

The field work allowed us to confirm most of the lineaments presented previously. These are generally shear corridors of variable orientation often containing shear bands and are locally intersected by veins and fractures or fault indicating various orientations. The shear corridors are marked by the development of schistosity on most formations and by foliation on the granitoids. Most of these ductile deformation structures are located within an angle of about 115° extending from N305°E to N60°E (Figure 3A). However, NNE-SSW to NE-SW structures are the most representative at the scale of the study area, while at the scale of Toega deposit we note a predominance of N-S to NNE-SSW structures. In summary, all these ductile deformation structures define three main orientations, separated by approximately 60°, corresponding to three directional families: G1 with a NW-SE orientation, G2 with a N-S orientation, and G3 with a NE-SW direction. The veins show a variable orientation; although at Toega deposit, N-S to NE-SW veins are predominant. Finally, the fractures and fault are mainly NW-SE direction but some are NNE-SSW.

 ISSN: 1857-7881 (Print) e - ISSN 1857-7431

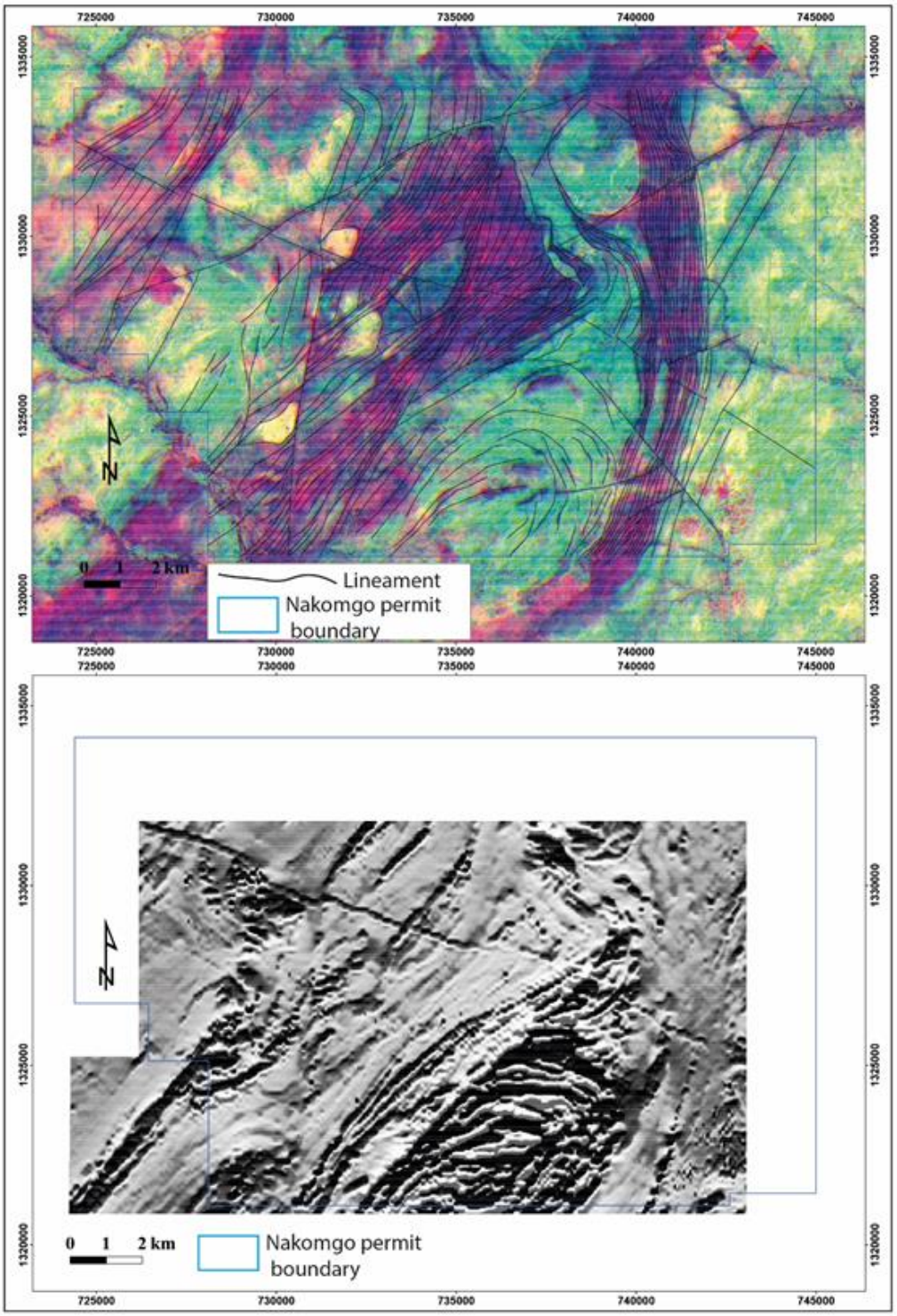

Figure 2. Lineaments map at Nakomgo permit scale
a: Lineaments tracing on Landsat 8 image background; b: Aeromagnetic image

 ISSN: 1857-7881 (Print) e - ISSN 1857-7431

G1 NW-SE Ductile Structures

The G1 structures are the least represented in the field. They mainly affect the orthogneiss and a few parts of the microgranite. They are shear corridors marked by a continuous schistosity with a general NW-SE orientation and a subvertical dip to the southwest and sometimes to the northeast. This schistosity carries a mineral lineation highlighted by the alignment of micas as well as a stretching lineation expressed by the stretching of the overmicaceous enclaves. These lineations dip slightly to the southeast. Microscopically, the continuous schistosity is marked by the alignment of micas and quartz sub-grains. It sometimes rolls up phenoclasts of feldspars and quartz as a pressure shadow. In some places, the NW-SE schistosity is taken up by a disjunctive schistosity isolating fragments like fish structure (Figure 4F-c).

G2 N-S Ductile Structures

They are visible on granites, meta-conglomerates, meta-sandstones, metadiorites, amphibolites, and metadolerites. These rocks generally outcrop as elongated mounds describing broad N-S trending shear zones and containing structures represented mainly by continuous schistosity or foliation with associated folds, boudins, and stretching lineation. The schistosity and foliation show a general N-S to NNE-SSW orientation with a strong dip to the SE. The first is characterized by a desquamation of the rock in a few millimeters and is observed in particular on the sedimentary deposits and the microgranite, whereas the second, more or less frustrated, affects the granitoids. At the limits of the shear corridors affecting the microgranite, the continuous schistosity follows the planes imbricate structure with an increasingly shallow dip.

 ISSN: 1857-7881 (Print) e - ISSN 1857-7431

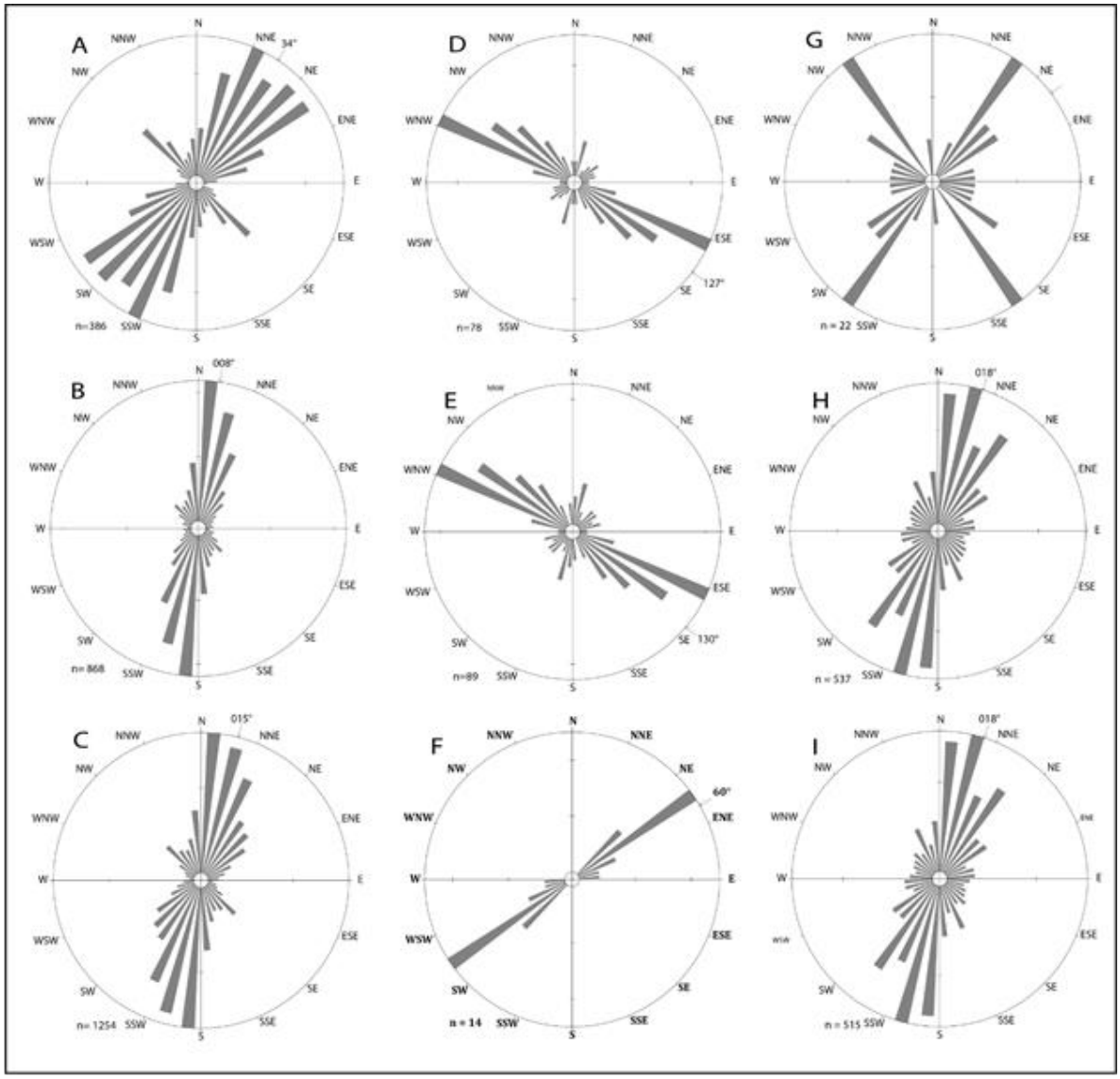

Figure 3. Rose diagrams of foliation/schistosity, fractures/faults and veins
Lines 1, 2, and 3 represent the structures at Nakomgo scale, Toega deposit, and both domains respectively. A, B, and C: Foliation/schistosity; D, E: Fractures/faults; F: Shear bands; G, H, I: veins

The lineation carried by the schistosity corresponds to the stretching of the porphyroclasts in the meta-sediments and to the stretching of the overmicaceous enclaves in the intrusive rocks. It is weakly plunging. As for the boudinage, it affects veins parallel to the N-S foliation in the form of symmetrical bodies.

 ISSN: 1857-7881 (Print) e - ISSN 1857-7431

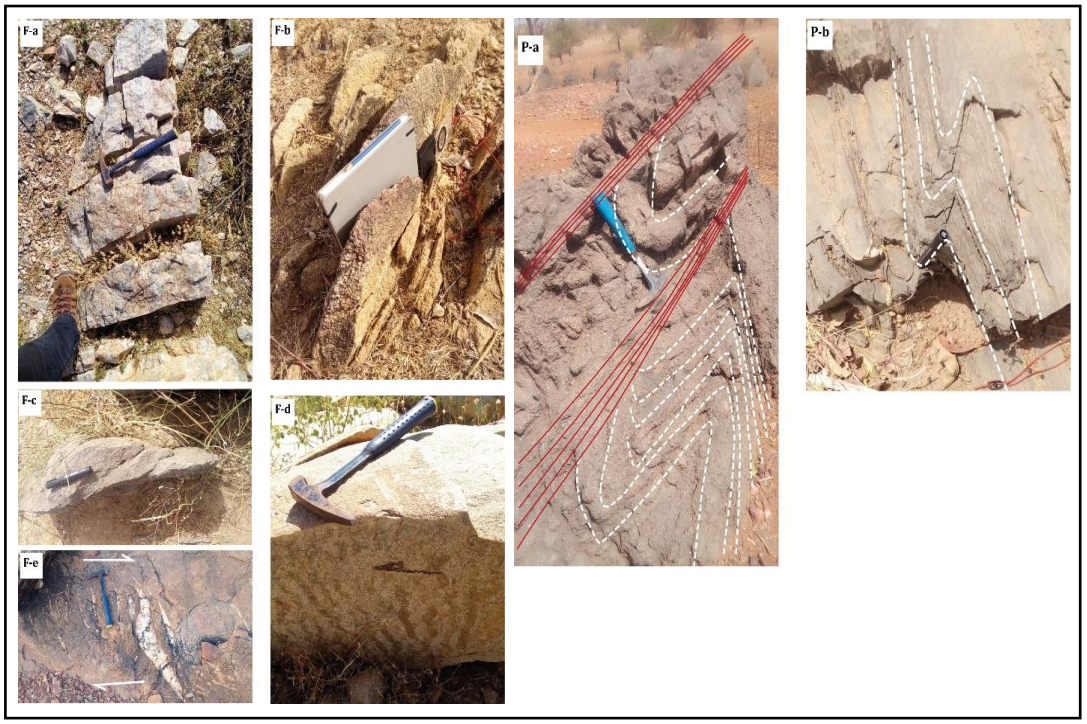

Figure 4. Examples of field structures. F-a, F-b: Disjunctive shistosity; F-c: Mylonitic shistosity; F-d: Strike-slip fault plane; F-e: en echelon tension gashes; P-a: Fold showing pointed hinges and intersected by shear bands; P-b: Dissymetric fold with subvertical axis.

Locally, the schistosity is associated with folds affecting the whole rock. These folds with a wavelength of about 80 cm sometimes show pointed hinges and subvertical axial planes with a NNE-SSW orientation (Figure 4P-a). They are taken up by centimeter-sized shear channels intersecting the axial planes at a low angle. Microscopically, the schistosity is highlighted by an alignment of micas sheets and bands of quartz sub-grains in the meta-sediments and sometimes by that of hornblende rods in the metadolerites. Within this ensemble formed by the micas sheets and quartz (Figure 11O-a and O-b), we note the presence of porphyroclasts of quartz totally recrystallized or not and drawing pressure shadows generally symmetrical. Locally, the schistosity is overprinted sometimes by shear bands sub-parallel to the schistosity, and sometimes by an oblique crenulation marked by thin shear bands intersecting the micro-folds. These are mylonitic zones.

G3 NE-SW Ductile Structures

They can be observed on almost all lithologies and are characterized not only by wide NE-SW shear zones but also by alternating very small NE-SW to ENE-WSW shear bands. The wide shear zones are marked by a continuous NE-SW trending schistosity dipping subvertically to the southeast

 ISSN: 1857-7881 (Print) e - ISSN 1857-7431

and sometimes to the northwest. This schistosity also contains a moderately northeast-dipping stretching lineation. In some places (Figure 4P-b), asymmetric folds showing pointed hinges and subvertical axial planes parallel to the schistosity are observed.

The shear bands are millimeter to centimeter strong and cut the continuous schistosity. The advent of these bands also caused the development of folds, asymmetrical boudins, and lineations. Generally, very laminated, the bands appear as a disjunctive schistosity showing a strong dip and are generally turned to the northwest. In the field, this schistosity often takes up earlier continuous schistosities isolating fusiform or lozenge-shaped rock fragments. These are mylonitic zones. Indeed, on the metadiorites (Figure 5M-a), the continuous N-S schistosity is affected by a disjunctive schistosity of NE-SW orientation and millimeter strength and angular deviation up to 30°.

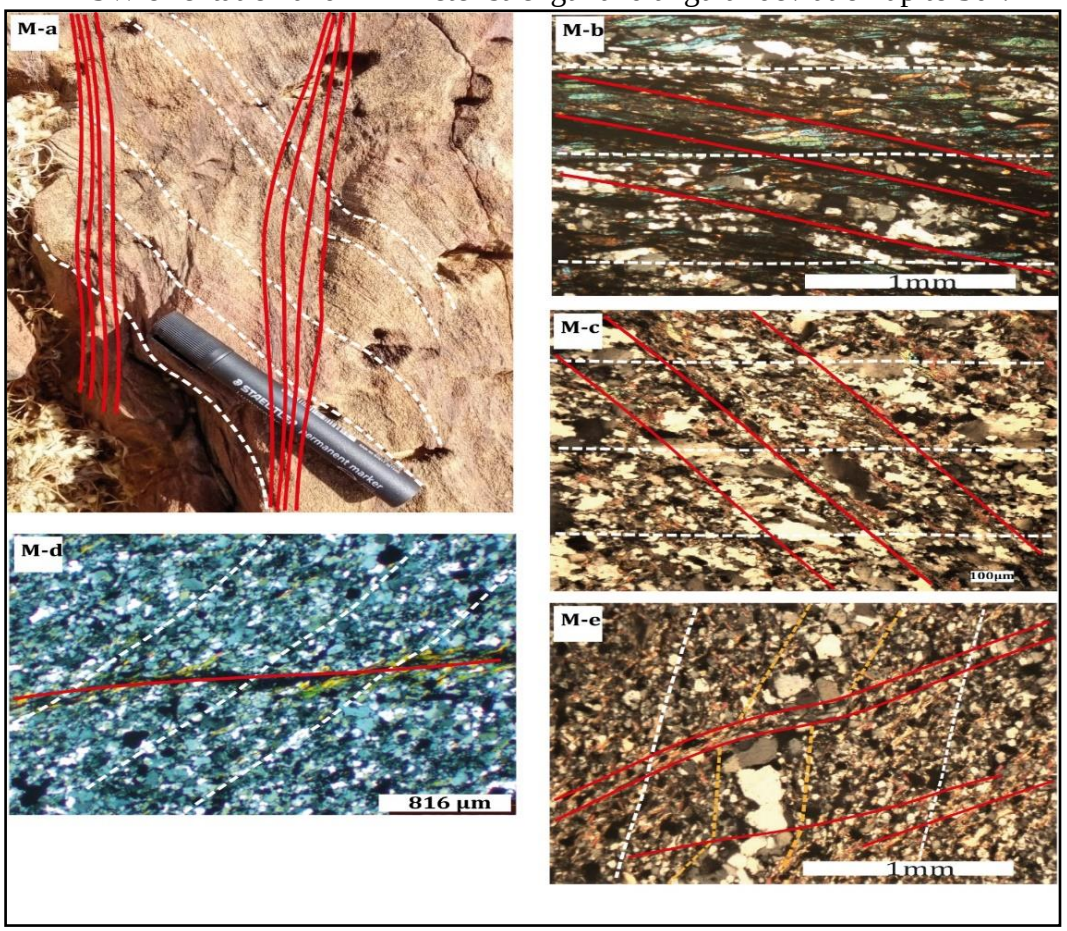

Figure 5. Macro and microphotography of mylonitic zones. M-a: Shear bands cutting N-S schistosity with a moderate angle; M-b: Shear bands cutting N-S schistosity with a low angle and showing biotite fish structures; M-c: Shear bands cutting foliation with high angle; M-d: Foliation deviation due to shear band; M-e: Shear bands cutting both foliation and quartz veinlet.

 ISSN: 1857-7881 (Print) e - ISSN 1857-7431

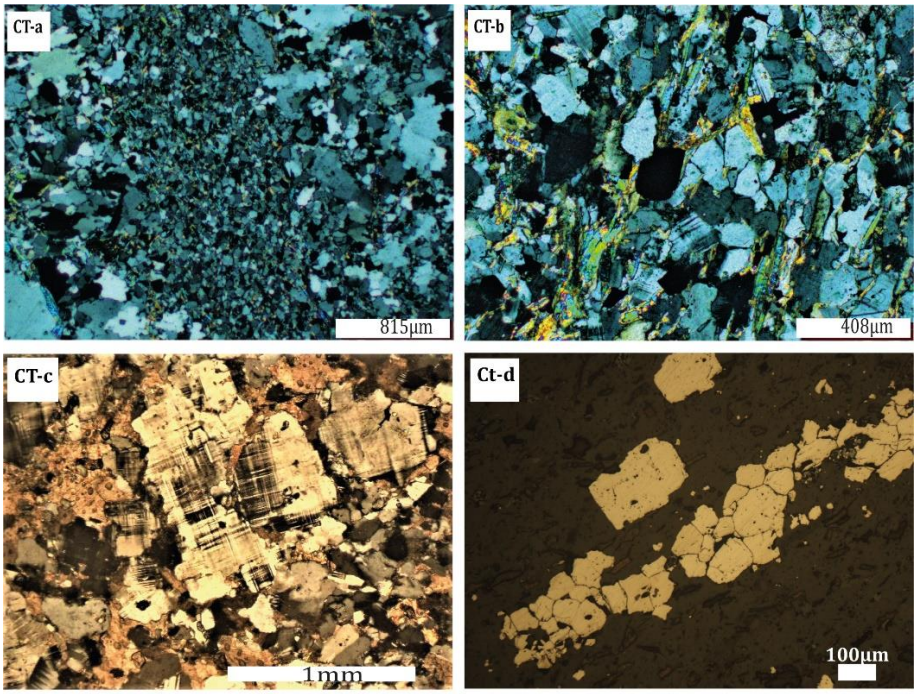

Figure 6. Microphotographs indicating some kinematic keys and cataclastic zones. B-a: Microboudinage of quartz veinlet indicating dextral sense; P-c & P-d: Dissymetric microfolds affecting mica clusters and showing dextral vergence; O-a: σ-type pressure shadow; CT-a & CT-b: Cataclastic structures developed in granite; CT-c: Fragmented micricline cystal; Ct-d: Band of fragmented pyrrhotite crystals.

This overprinting is also observed within the NE-SW shear (Figure 5M-b and M-c) where the SE dipping NE-SW continuous schistosity is cut by a NE-SW to ENE-WSW disjunctive schistosity. Locally, on the microgranite, the NE-SW disjunctive schistosity has resulted in the development of crenulation marked by the alignment of the axes of the microfolds perpendicular to the NW-SE continuous schistosity. Shear bands are also visible on the rock cores (Figure 5M-d; Figure 6B-a) and are marked by lamination resulting in oblique crenulation, foliation deviation, and vein boudinage. Folded sections, generally of variable size, are present. They (Figure 6P-c and P-d) generally affect the mica clusters and quartz veinlets and clearly show alternating long and short limbs. They are dissymmetric and sometimes disharmonic folds, especially those affecting the veinlets.

Microscopically, and in the case of microgranites and meta-sediments (Figure 5M-e and Figure 6B-a), the disjunctive schistosity is clearly expressed as shear affecting the mica bands and sometimes intersecting the quartz veins parallel to the continuous schistosity, sometimes forming asymmetrical microboudinage or vein strike-slip. Locally, it overlies the continuous schistosity and forms an oblique to sub-perpendicular crenulation. Finally, this

 ISSN: 1857-7881 (Print) e - ISSN 1857-7431

shearing is also responsible for a lamellar deformation of quartz and a fragmentation of feldspars and some opaques into small bodies, which are often pyramidal delimiting cataclastic zones (Figure 6CT-a to CT-b).

Brittle-Ductile Structures and Fractures

A few brittle-ductile structures were observed on several outcrops and on the rock cores. These are notably tension gashes. These are generally sigmoidal and grouped en echelon (Figure 5F-e) with a general orientation N145°E. Other evidence of brittle-ductile deformation appears microscopically as damaged zones in meta-sediments and cataclastic zones in granites.

Fractures (Figure 5F-a and F-b) are very common in the field. They are observable across all lithologies and show a preferential major WNW-ESE and secondary NNE-SSW to NE-SW orientation (Figure 4D and E). Most of them show subvertical dips. These structures often occur as two planes of disjunctive schistosity separating variable size microlithons. Some of them are faults without neomineral filling but marked by the presence of a fault mirror (Figure 5F-d). They sometimes follow the NW-SE and sometimes the NE-SW schistosity planes. Other faults expressed by the offset of quartz veins show various orientations.

Mineralization

Mineral exploration in the region has revealed the presence of gold mineralization at Toega zone. The deposit extends over 1200 meters and is 430 meters wide. Inferred mineral resources are estimated at 22 million tons of ore with an average grade of 1.9 g/t gold (West African Resources, 2023). This mineralization is located in a N-S shear zone. Analysis of assay data from the drill holes, visualized as sections, shows that the mineralization begins at a depth of about 20 meters and plunges eastward to a depth of over 200 meters. In order to better characterize the mineralization, samples were taken from the mineralized slices, the waste rock zones that they intersect, and from those that surround the mineralization. The petrographic and metallographic observations show that this mineralization is essentially carried by the amphibole microgranite and metasediments, particularly within its cataclastic portions marked by a fragmentation of the main minerals into small bipyramidal bodies, as well as by a crushing of the chalcopyrite. Within these zones, gold is both disseminated in the rock and carried by deformed quartz veinlets. In waste rock, chalcopyrite is rare and results mainly from stretched pyrrhotite which is very common.

 ISSN: 1857-7881 (Print) e - ISSN 1857-7431

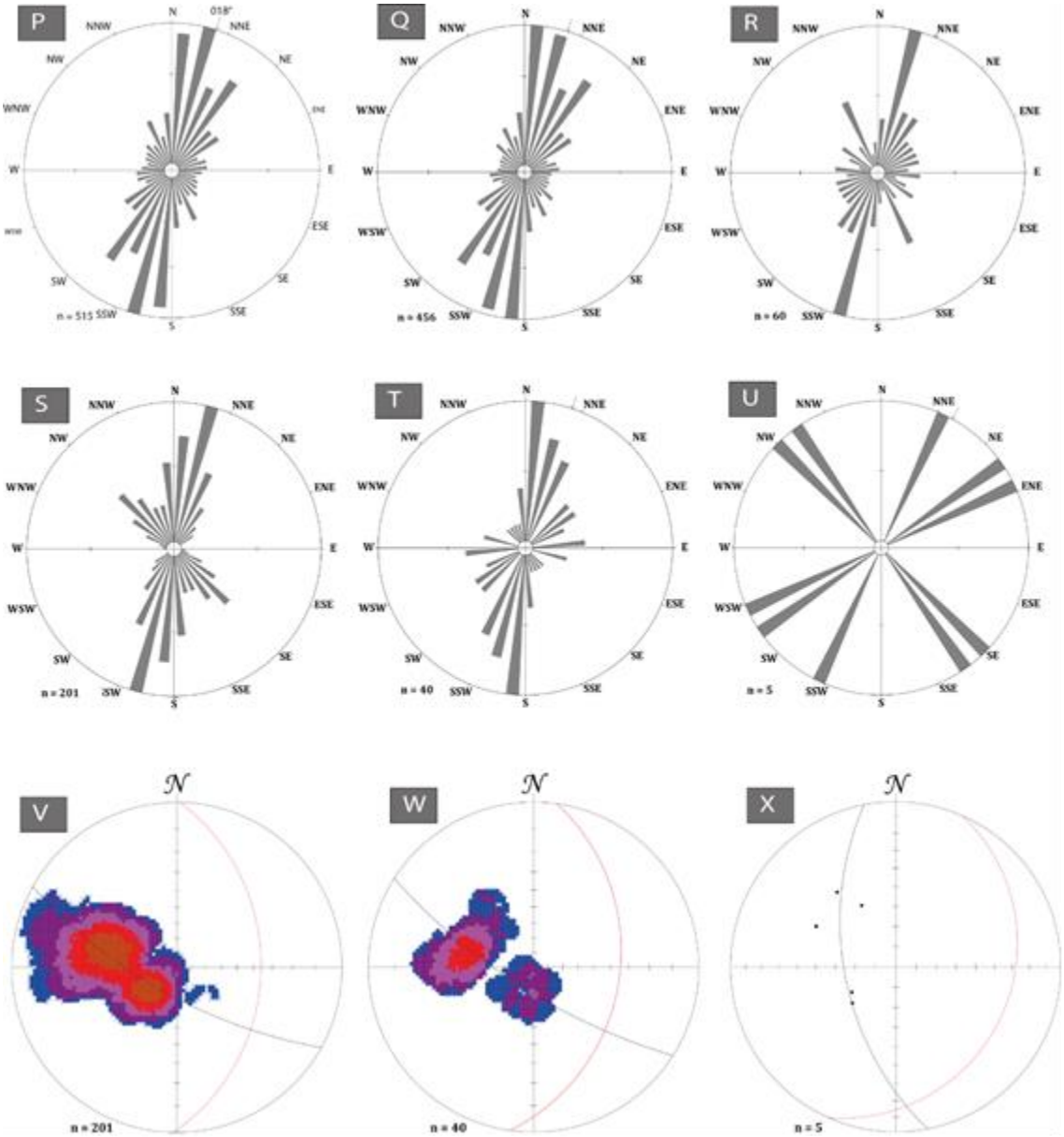

Figure 7. Rose diagrams of structures took in mineralized and barren zones at Toega deposit P, Q & R: Direction of veins at Teoga deposit, in sterile and mineralized area respectively; S, T & U: Direction of foliation in sterile zones, low grade (gold grade < 2g/t) and high grade (gold grade > 2g/t) mineralized domains respectively; V, W & X: Evolution of the main direction (red line) of the foliation in sterile zones, low grade (gold grade < 2g/t) and high grade (gold grade > 2g/t) mineralized domains respectively.

Structural analysis shows that the mineralized zone is marked mainly by a N-S to NNE-SSW foliation. The NE-SW and NW-SE foliations are weakly represented. In general, the veins have the same direction as the

 ISSN: 1857-7881 (Print) e - ISSN 1857-7431

foliation. However, there is a relative increase in the proportion of NW-SE veins if we consider only the mineralized ones. In addition, their average orientation turns slightly to the east compared to the barren veins (Figure 7P to R). Furthermore, a zoom on the behaviour of the foliation in the mineralized and barren passes shows that (i) in the barren levels (gold grade less than 0.1 ppm), the foliation maintains its N-S orientation, (ii) in the weakly mineralized passes (gold grade between 0.1 ppm and 2 ppm), the foliation shows a slight deviation towards the east and (iii) in the high-grade zones (gold grade higher than 2 ppm), it deviates more towards the east to take NNE-SSW direction (Figure 7S to W). In all three cases, the dip direction remains the same. Finally, the only faulted structure that we were able to measure on the cores follows the NNE-SSW direction parallel to the foliation in the last case.

Discussion

Finite Deformation Analysis

Finite deformation analysis is used to discuss the tectonic history within a region using deformation markers. The main markers we have selected for this purpose are lineation carried by foliation and fault mirrors, pressure shadows, microboudins, microfolds, and shear band cleavages. These features are good indicators of shear sense (Passchier & Rodolph, 2005) and are commonly used to define deformation kinematics. We have only considered those observed in the (X, Z) and (Y,Z) planes. With respect to lineation, measurements were made on the stretching lineations contained on the NW-SE and NE-SW schistosity planes and on the striations found on the fault mirrors that are parallel to each of these shear zones. Ten measurements were made in the NW-SE corridors and eight in the NE-SW shear zones. These measurements were made from the line bearing planes and their pitch. The results of these measurements shown on the stereogram (Figure 11Ln) indicate that all lines carried by the NW-SE continuous schistosity are weakly dipping (~ 25°) to the SE and of NW-SE azimuth. Their movement calculated from the polar of the bearing plane and the line draws a sinistral sense. This results in a decrease of orientation of the bearing plane of the fault/schistosity polar and the line relative to the orientation of the fault/schistosity itself. This plane is called fault movement and the average reduction in its orientation is about -5°. On the other hand, the lineations in the NE-SW corridors are moderately dipping (~30°) towards the northeast. Moreover, their movement describes a clockwise rotation. This first analysis shows that the two shear zones are moving in opposite directions. Pressure shadow analysis in both shear zones supports this conclusion. Indeed, both corridors contain sigma-type pressure shadows showing an asymmetric geometry (Figure11O-C and O-d) reflecting NW-SE sinistral shearing and NE-SW dextral shearing. In addition, microboudins (Figure 6B-a) and microfolds (Figure 6P-c and P-d) occurring

 ISSN: 1857-7881 (Print) e - ISSN 1857-7431

in the NE-SW shear zones also show asymmetric or dissymmetric geometry, which indicates a simple shear dextral movement. However, the pressure shadows and microboudins described in the N-S shearing (Figure 11O-a and O-b) are generally symmetrical and reflect coaxial deformation. The first are sigma-like, while the second are characterized by segmentation of quartz veins parallel to the continuous schistosity into stretched and symmetrical fragments. In addition, the N-S and NE-SW shear zones are marked locally by the development of mylonitic zones within which we observe a shear band cleavage characterized by a superposition of C type shear band to the S type cleavage. The shear bands, generally outlined by bands of oxidized or unoxidized micas, intersect the continuous schistosity marked by the alignment of biotite-sericite beds. This often results in the arrangement of the latter into fusiform bodies (as shown in Figure 5M-b), commonly referred to as mica fish. In mylonitic microgranites, shear bands draw opposite curves at their extremities that characterize deviation of the foliation. In all cases, the angular deviation between these two structures (Figure 5) is sometimes very small (less than 20°), and sometimes large (more than 60°). The analysis of the geometry of these micas fish and deviation of the foliation shows a dextral movement.

 ISSN: 1857-7881 (Print) e - ISSN 1857-7431

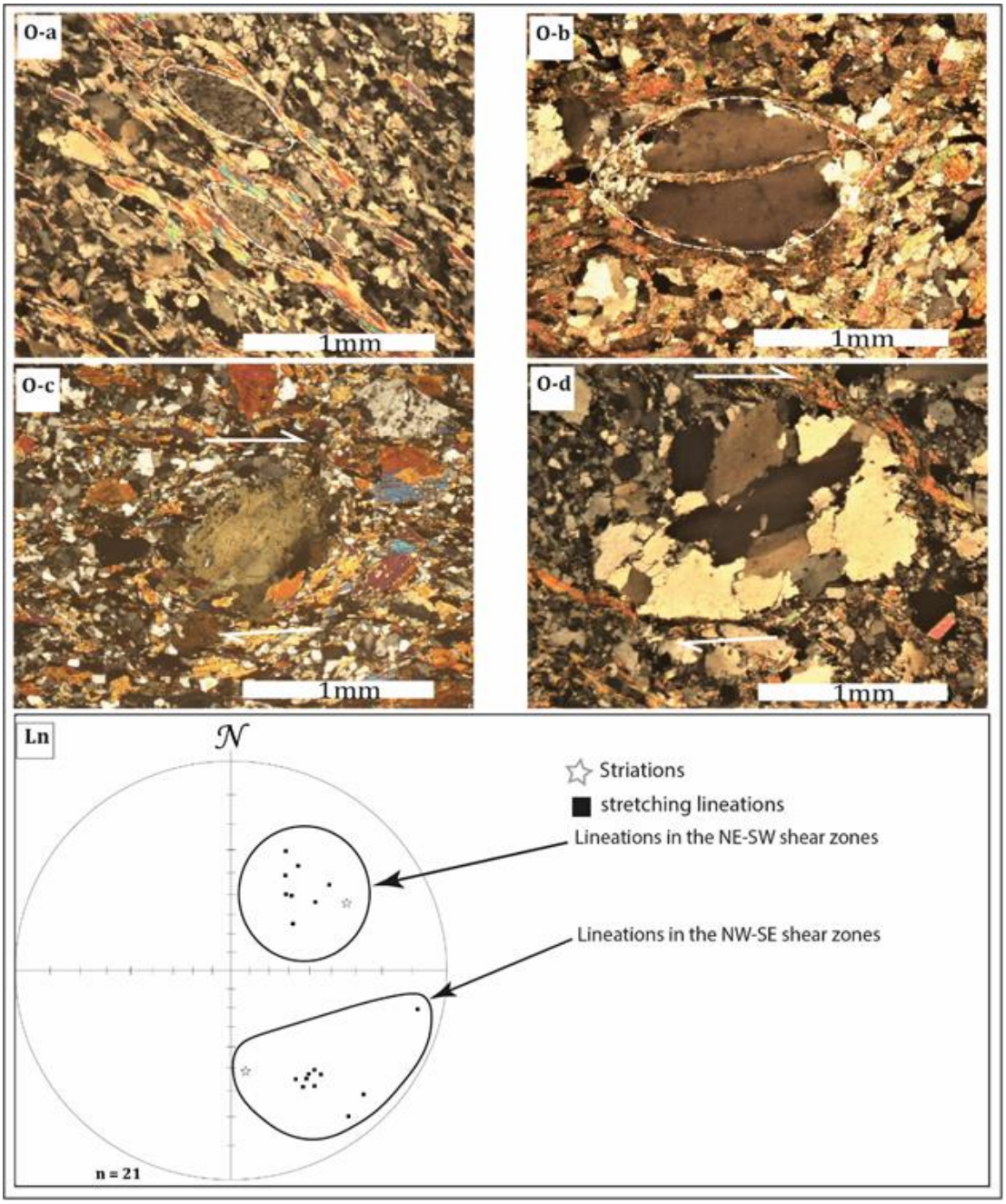

Figure 8. Microphotographs and stereogram. O-a & O-b: Symmetrical pressure shadows; O-c & O-d: Asymmetrical pressure shadows showing dextral sense; Ln: Stereogram of lineations.

However, we have noted the presence of shear bands arranged perpendicular to the continuous NW-SE schistosity and affecting the microgranites in some places. This patterning highlights perpendicular

 ISSN: 1857-7881 (Print) e - ISSN 1857-7431

crenulation and is evidence that the advent of the shear bands postdates the NW-SE shear zones.

Deformation Evolution

According to the above, the evolution of deformation in this part of Burkina Faso was initiated by the establishment of NW-SE shear zones due to NE-SW shortening. The weakly southeast-dipping lineations that these zones host, clearly different from the moderately northeast-dipping lineations carried by the NE-SW corridors, as well as the quasi-perpendicular superimposition of the shear bands on the continuous NW-SE schistosity, support this idea. Similar structures have already been observed in northern Burkina Faso and interpreted as early structures (Tshibubudze *et al.*, 2009; 2013; 2016; Hein *et al.*, 2010; McCuaig *et al.*, 2016) formed during the pre-Eburnean period called Tangaen. Furthermore, similar structures have been described in the southern region of the country by Baratoux et al. (2011), believed to have formed due to N-S Eo-Eburnean shortening. In addition, in northern Ghana, close to this study area, sinistral shear zones have been observed (Block *et al.*, 2016) and interpreted as the early structures in this locality. However, the work of Fontaine *et al.* (2017) conducted in the same area as this study could not reveal the existence of such early structures. According to their findings, the tectonic history in this part of the country started with the E-W compression, responsible for the development of the N-S structures, and ended with the setting of the N010°E and N100°E faults. The work of Saga *et al.* (2021) carried out in the same area of Zorgho based on the interpretation of aeromagnetic images and field mapping revealed the existence of a NW-SE to NNW-SSE shear zone called Tanlouka shear zone and marked by mylonitic schistosity and sub-parallel fractures. However, according to the authors, the concomitant emplacement of these two ductile and brittle structures is related to the local change in rheological conditions and marks the end of tectonic events in this locality.

The E-W horizontal shortening subsequently led to the development of N-S corridors. These corridors contain symmetrical pressure shadows and boudins that indicate coaxial shearing. Similar oriented corridors have been recognized in several localities in Burkina Faso (Woodman *et al.*, 2015; McCuaig *et al.*, 2016; Fontaine *et al.*, 2017), although the kinematics of the deformation are not always established. This highly localized flattening in our study area precedes transcurrent deformation marked by non-coaxial dextral shear having occasioned the development of NE-SW shear zones overlaid late by NE-SW to ENE-WSW shear bands. The asymmetry of pressure shadows, microfolds, microboudins, as well as the fish structures related to the shear band cleavages, reflect this style of deformation. The advent of NE-SW shear corridors is the most pronounced tectonic event across the Paleoproterozoic

 ISSN: 1857-7881 (Print) e - ISSN 1857-7431

basement of the Baoulé/Mossi domain and Burkina Faso (Allibone *et al.*, 2002; Castaing *et al.*, 2003; Naba *et al.*, 2004; Feybesse *et al.*, 2006; Baratoux *et al.*, 2011; Metelka *et al.*, 2011; Fontaine *et al.*, 2017; Murray *et al.*, 2019; Chardon *et al.*, 2020). In addition, structures resembling the shear bands we have described were also observed. As the principal stress clockwise rotates, the crust acquires ductile-brittle behavior marked by the emplacement of ductile-brittle structures and then by the opening of strike-slip faults. These faults show two preferential orientations. The main one varies from WNW-ESE to NW-SE, corresponding to an angular deviation of about 70° with respect to the shear bands. Such faults indicate sinistral movement. The second, weakly represented, indicates dextral movement and NNE-SSW orientation at about 70° also with respect to the shear bands. This architecture appears to be the result of progressive deformation. The work of Saga *et al.* (2021) supports this thesis because the authors interpreted the late opening of the NW-SE fractures as the result of a continuum deformation, which would be consistent with progressive deformation.

Structural Model

Several studies conducted across the Man/Léo Ridge and Burkina Faso tend to explain the anastomosing structural architecture observed in the Paleoproterozoic basement by the result of a combination of several tectonic phases often marked by inversions of the position of the main stress (Allibone *et al.*, 2002; Feybesse *et al.*, 2006; Hein *et al.*, 2010; Ouiya *et al.*, 2015; Woodman *et al.*, 2015; Sawadogo *et al.*, 2021; Siagné *et al.*, 2022). However, these studies have not yet established the origin of these multiple inversions. These studies deviate from the hypothesis of a common genetic relationship explaining the occurrence of all observed structures, although this has been observed elsewhere (Tchalencko & Ambrassey, 1970; Khodayar et al., 2018). This proposed model views all of the ductile and brittle structures observed in this part of the country except for the early NW-SE shear zones as the result of progressive deformation extending from early Eburnean times to the present. We argue for simple dextral shearing in which the dominant normal component at the beginning generated an E-W constriction resulting in the emplacement of the N-S shear zones. Subsequently, the simple shear component took over, resulting in the development of the dominant NE-SW dextral shear zones. As the dextral shear movement evolved, the initiation of NE-SW to ENE-WSW shear bands is noted. These structures intersect the NE-SW zones at a low angle (~20°) and would correspond to the synthetic Riedel R structures with respect to their dextral movement. The latter intercept sinistral WNW-ESW strike-slip faults with a high degree (~70°) equivalent to Riedel antithetic R' structures, and dextral NNE-SSE faults with a high degree equivalent to Chalenko's P structures. This structural model (Figure 9) is close

 ISSN: 1857-7881 (Print) e - ISSN 1857-7431

to some already interpreted in Archean provinces in North America (Hudleston *et al.,* 1988; Robert,1990), and in the vicinity of the san Andreas Fault (Sylvester & Smith, 1976) and taken up recently by some authors (Fossen, 2016; David *et al.*, 2018; Khodayar et al., 2018; Velasquez, 2018).

The geodynamic conditions that can generate this structural architecture can be derived from the work of Chardon (2020). Indeed, the study area is located in domain 1 of Chardon (2020). This domain is bounded to the west by the Ouahigouya shear zone. The dextral movement of this corridor would have caused the progressive clockwise rotation of this block and the development of the N-S to ENE-WSW ductile structures and NNE-SSW to WSW-ENE brittle structures.

The observation of the tension gashes, although localized, allows us to propose the orientation of the stress that caused their development. As a reminder, *en échelon* veins have a general orientation of N145°E. This assumes the same direction for the main stress. On the other hand, the bisector of the acute angle between the synthetic R structures and antithetic R' which, according to Tchalenko and Ambrasey (1970), indicates the orientation of the main stress is at approximately N100°E, that is to say an angular deviation of 45°. This angular deviation, which seems to be important, can be explained by the more or less late emplacement of some granitoids which would have caused a local deviation of some structures.

Implication for Gold Mineralization

The Toega deposit is located in a N-S shear corridor marked by a strongly east-dipping N-S foliation affecting both sedimentary deposits and granites. This corridor also hosts the NW-SE foliation, which is weakly represented but reflects an intersection of the two shear corridors and is superimposed by the NE-SW structures. This corroborates with the work of Tshibubudze *et al.* (2015) who revealed that the Essakane deposit is located at the intersection between the early NW-SE thrust structures and the NE-SW shear corridors. It also illustrates the fact that across the Léo Ridge, most of the deposits discovered on the Paleoproterozoic basement are located along shear corridors and associated relay structures (Feybesse *et al.,* 2006; Dubé & Gosselin, 2007; Augustin *et al.,* 2017; Murray *et al.,* 2019; Chardon *et al.,* 2020).

 ISSN: 1857-7881 (Print) e - ISSN 1857-7431

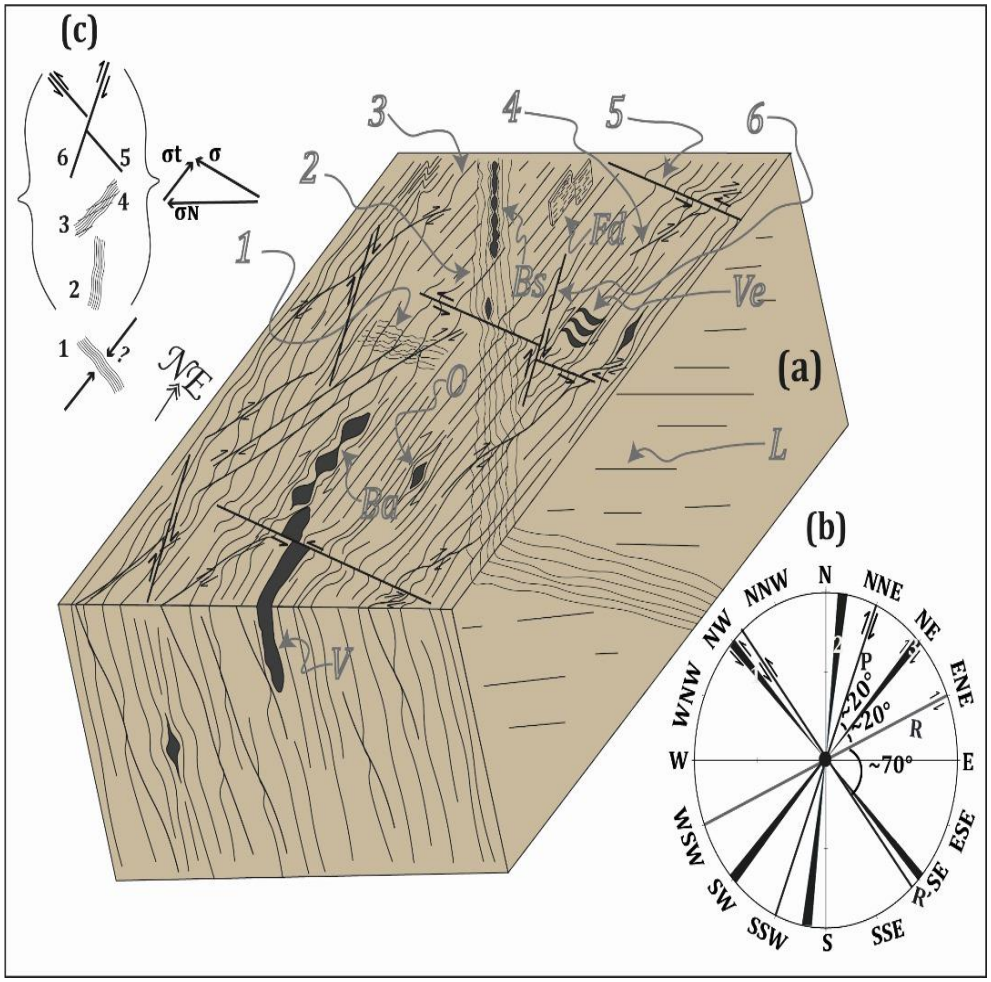

Figure 9. Structural model at Nakomgo permit. (a) Block model indicating the main structures; (b) Rose diagram showing directional relationship between the structures; (c) Simplified relationship between tresses and the structures (σ is the main stress; σ_N the normal stress and σ_t the shearing stress). 1: NW-SE sinistral shear zone; 2: N-S Shear zones; 3: NE-SW dextral shear corridors; 4: ENE-WSW dextral shear bands (R type structure); 5: Sinistral strike-slip fault (R' type structure); 6: Dextral strike-slip fault (P type structure); V: Quartz veins; Ba: Asymmetrical boudin; Bs: Symmetrical boudin; Fd: Fold; O: Pressure shadow; Ve: In echelon veins; L: Lineation

Most of the formations affected by these shears, notably the NW-SE non-coaxial and N-S coaxial deformations, show hydrothermal alteration highlighted by the recurrent and disseminated presence of pyrrhotite. On the other hand, at the scale of the permit, we have noticed that all lithologies showing only the markers of the dextral NE-SW shear are waste. Therefore, the tectonic events responsible for the development of the early NW-SE shear zones, notably the N-S shear zones, would also be synchronous with the gold mineralization at Toega. Woodman (2015) and McCuaig (2016) had

 ISSN: 1857-7881 (Print) e - ISSN 1857-7431

previously reached similar results in southern and northern Burkina Faso respectively.

However, the increase in gold mineral concentrations, as the structures clockwise rotation shows that dextral transcurrent shear, notably brittle-ductile deformation, played a crucial role in the remobilization and precipitation of gold fluids. Indeed, in the barren zones, the dominant structures are N-S. They take NNE-SSW orientation in the weakly mineralized zones and then NE-SW to ENE-WSW in the highly mineralized sections. The latter orientation is parallel to the direction of the shear bands and the dextral strike-slip faults but secants the WNW-ESE faults. This is consistent with the results of the work of David *et al.* (2018) who showed that at the district or deposit scale, gold mineralization is associated with a variety of faults and shear zones formed prior to the mineral episode but remains completely confined between sub-parallel relay fracture pairs intersecting the early structures. Gold concentrations would be emplaced in the dilation zones created within the blocks exposed by the early structures.

In addition, the zones hosting the mineralization show cataclasic conditions characterized by fragmentation or even crushing of the minerals, including chalcopyrite-type sulphides. Furthermore, most of the mineralized veins are NNE-SSW and NW-SE trending and are covered by NE-SW to ENE-WSW shear bands. These markers of ductile-brittle deformation provide evidence that this type of deformation facilitated circulation and precipitation of gold-bearing fluids (Lompo, 2001; Béziat *et al.*, 2008; Baratoux *et al.*, 2015; Markwitz *et al.*, 2016).

The presence of mineralization in different rock types affected by coaxial deformation and intersected by dextral shearing, as well as the increase in gold grades with clockwise rotation of the structures, coupled with the fact that the mineral concentrations are exclusively located in the more or less crushed passes and in the deformed veins, seems to be evidence that mineralization is closely related to deformation. The Toega deposit can therefore be classified as an orogenic-type deposit where ductile-brittle deformation marking the end of tectonic events played a crucial role in the remobilization and concentration of gold-bearing fluids.

Conclusion

Two major tectonic events occurred in the central part of Burkina Faso. The first is the result of NE-SW shortening which probably occurred during the pre-Eburnean period. It is characterized by the development of sinistral NW-SE shear corridors that are locally preserved in the field as small pointed bodies. The second took place during Eburnean period. It corresponds to a transcurrent tectonics whose clockwise rotation generated the progressively ductile and brittle structures organized according to the Riedel-Tchalenko

 ISSN: 1857-7881 (Print) e - ISSN 1857-7431

model. At the beginning of this event, the E-W normal component of the main stress was responsible for the formation of N-S coaxial shear zones. Subsequently, the tangential component took over, causing the progressive development of non-coaxial NE-SW shear zones. These zones describe a dextral movement. As the crust progressively cooled, thin ENE-WSW shear bands, corresponding to synthetic R structures, and sinistral strike-slip faults, corresponding to R' structures, developed almost simultaneously. The development of dextral strike-slip faults associated with P-type structures would mark the end of this event.

The metallographic study reveals that the first event, as well as the E-W shortening that marks the beginning of the progressive deformation, are synchronous with the gold mineralization. In all cases, the development of synthetic R structures, coupled with brittle-ductile deformation, played a crucial role in the remobilization, concentration, and structuring of the ore bodies forming the Toega deposit.

Acknowledgement

This work was made possible by the assistance of the West African Resources Company, to whom we are grateful. In particular, we thank National Manager and geologist staff.

Conflict of Interest: The authors reported no conflict of interest.

Data Availability: All of the data are included in the content of the paper.

Funding Statement: The authors did not obtain any funding for this research.

References:

1. Andrew Allibone, H. (2002). Structural Controls on Gold Mineralization at the Ashanti Gold Deposit, Obuasi, Ghana. *Society of Economic Geologists, Special Publication 9, 2002, p. 65–93*
2. Andrew Tunks, J., David Selley, Jamie Roger, R., & Gary Brabham (2004).Vein mineralization at the Damang Gold Mine, Ghana: controls on mineralization. Journal of Structural Geology 26 (2004) 1257-1273. doi:10.1016/j.jsg.2003.11.005.
3. Augustin, J., Gaboury, D., & Crevier, M. (2017). Structural and gold mineralization evolution of the world-class orogenic Mana District, Burkina Faso: multiple mineralizing events over 150 million years., Ore Geology Reviews, 2017.
4. Baratoux, L., Metelka, V., Naba, S., Jessell, M., Grégoire, M., & Ganne, J. (2011). Coeval shortening of juvenile Paleoproterozoic oceanic arc crust and granitoid emplacement during the Eburnean

 ISSN: 1857-7881 (Print) e - ISSN 1857-7431

orogeny (~2.2–2.0 Ga): the Boromo, Houndé, and Banfora greenstone belts, western Burkina Faso. Precambrian Res. 191, 18–45.

5. Baratoux, L., Metelka, V., Naba, S., Ouiya, P., Siebenaller, L., Jessell, M.W., Nare, A., Béziat, D., Salvi, S., & Franceschi, G. (2015). Tectonic Evolution of the Gaoua Region: Implications for the Mineralization. Journal of African Earth Sciences xxx (2015) xxx-xxx. http://dx.doi.org/10.1016/j.jafrearsci.2015.10.004.
6. Béziat, D., Dubois, D., Debat, P., Nikiéma, S., Salvi, S., & Tollon, F. (2008). Gold metallogeny in the Birimian craton of Burkina Faso (West Africa). Journal of African Earth Sciences 50 (2008) 215-233. doi:10.1016/j.jafrearsci.2007.09.017.
7. Block, S., Jessell, M., Aillères, L., Baratoux, L., Bruguier, O., Zeh, A., Bosch, D., Caby, C., & Mensah, C. (2016). Lower crust exhumation during Paleoproterozoic (Eburnean) orogeny,NW Ghana, West African Craton: Interplay of coeval contractional deformation and extensional gravitational collapse. Precambrian Research 274 (2016) 82–109. http://dx.doi.org/10.1016/j.precamres.2015.10.014.
8. Boher, M., Abouchami, W., Michard, A., Albarède, F., & Arndt, T.N. (1992). Crustal Growth in West Africa at 2.1 Ga. Journal of Geophysical Research, vol, 97, NO. B1, Pages 345-367, January 10, 1992
9. Castaing, C., Bila, M., Milési, J-P., Thiéblemont, D., Le Metour, J., Egal, E., Donzeau, M.,Guerrot, C., Cocherie, A., Chevremont, P., Teygey, I., Itard, Y., Zida, B., Ouédraogo, I.,Koté, S., Kaboré, B.E., Ouédraogo, C., Ki J-C., & Zunino, C. (2003). Notice explicative dela carte géologique et minière du Burkina Faso à 1/1000 000. 3ème édition: 1-148
10. Chardon, D., Bamba O., & Traoré, K. (2020). Eburnean deformation pattern of Burkina Faso and the tectonic significance of shear zones in the West African craton. BSGF-Earth Sciences Bulletin 2020, 191, 2. https://doi.org/10.1051/bsgf/2020001
11. David, I. G., Santosh, M., Richard, J. G., & Liang, Z. (2018). Structural geometry of orogenic gold deposits: Implications for exploration of world-class and giant deposits. Geoscience Frontières 9 (2018) 1163-1177. https://doi.org/10.1016/j.gsf.2018.01.006
12. Dubé, B. & Gosselin, P. (2007). Greenstone-hosted quartz-carbonate vein deposits, *in* Good fellow, W.D., ed., Mineral Deposits of Canada: A Synthesis of Major Deposit-Types, District Metallogeny, the Evolution of Geological Provinces, and Exploration Methods: Geological Association of Canada, Mineral Deposits Division, Special Publication No. 5, p. 49-73.

 ISSN: 1857-7881 (Print) e - ISSN 1857-7431

13. Ducellier, J. (1963). Contribution à l'étude des formations cristallines et métamorphiques du Centre et du Nord de la Haute Volta. Mém. B.R.G.M., Paris, 312, pp.769-776.
14. Ferré, E. C. & Caby, R. (2007). Granulites facies metamorphism and charnokite plutonism: examples from the Neoproterozoïc belt Northern Nigeria. Proceedings of Geologists Association 18, 1-8.
15. Feybesse, J., Billa, M., Guerrot, C., Duguey, E., Lescuyer, J., Milesi, P., & Bouchot, V. (2006). The paleoproterozoic Ghanaian province: Geodynamic model and ore controls, including regional stress modeling. Precambrian Research 149 (2006) 149-196. doi:10.1016/j.precamres.2006.06.003
16. Fontaine, A., Eglinger, A., Ada, K., André-Mayer, S., Reisberg, L., Siebenaller, L., Le Mignot, E., Ganne, J., & Poujol, M. (2017). Geology of the world-class Kiaka polyphase gold deposit, West African Craton, Burkina Faso Journal of African Earth Sciences 126 (2017) 96-122 http://dx.doi.org/10.1016/j.jafrearsci.2016.11.017
17. Haakon, F. (2016). Structural geology. Second edition, Cambridge University Press
18. Hein, K. A. A., Morel, V., Kagone, O., Kiemde, F., & Mayes, K. (2004). Birimian lithological succession and structural evolution in the Goren Segment of the Boromo-Goren Greenstone Belt, Burkina Faso. Journal of African Earth Sciences 39, 1–23.
19. Hein, K. A .A. (2010). Succession of structural events in the Goren greenstone belt (Burkina Faso): Implications for West African tectonics. Journal of African Earth Sciences 56 (2010) 83-94. doi:10.1016/j.jafrearsci.2009.06.002.
20. Hottin, G. & Ouédraogo, O. F. (1976). Carte géologique du Burkina Faso au 1/1000000ème, 2ème ed., 1992, Bureau des mines et de la géologie du Burkina Faso.
21. Hudleston, P.J., Schultz-Ela, D., & Southwick, D. L. (1988). Transpression in an Archean belt, northern Minnesota. Canadian Journal of Earth Sciences; volume 25, pages 1060- 1068.
22. Kagambèga, N., Lompo, M., Diallo, D. P., & Naba, S. (2004). Les granitoïdes paléoprotérozoïques du Burkina Faso (Afrique de l'Ouest) - Caractères pétrologiques. J. Sci. Vol. 4, n°3, Dakar, Sénégal, pp : 81−96.
23. Khodayar, M., Bjornsson, S., Kristinsson, S.G., Karlsdottir, R., Olafsson, M. & Vikingsson, S. (2018). Tectonic Control of the Theistareykir Geothermal Field by Rift and Transform Zones in North Iceland: A Multidisciplinary Approach. Open Journal of Geology, 8, 543-584. https://doi.org/10.4236/ojg.2018.86033

 ISSN: 1857-7881 (Print) e - ISSN 1857-7431

24. Lompo, M., Caby, R., & Robineau, B. (1991). Evolution structurale du Birimien au Burkina Faso-exemple de la ceinture de Boromo-Goren dans le secteur de Kwademen (Afrique de l'Ouest). Comptes Rendus de l'Académie des Sciences, Paris 313, 945-950.
25. Lompo, M. (2001). Le paléoprotérozoïque Birimien du Burkina Faso -Afrique de l'Ouest- Evolution crustale et concentrations aurifères. Mémoire d'Habilitation à Diriger des Recherches
26. Lompo, M. (2009). Geodynamic evolution of the 2.25-2.0 Ga Paleoproterozoic magmatic rocks in the Man-Leo Shield of the West African Craton. A model of subsidence of an oceanic plateau (Eds), Paleoproterozoic Supercontinents and Global Evolution, vol. 323. Geological society of London, Spécial Publiscations, pp. 231-254.
27. Lompo, M. (2010). Paleoproterozoic structural evolution of the Man-Leo Schield (West Africa). Journal of African Earth Sciences 58 (2010) 19-39
28. Markwitz, V., Hein, K.A.A., Jessell, M., & Miller, J. (2015). Metallogenic portfolio of the West Africa craton. Ore Geology Reviews (2015). http://dx.doi.org/10.1016/j.oregeorev.2015.10.024
29. Markwitz, V., Hein, K.A.A., & Miller, J. (2016). Compilation of West African mineral deposits: Spatial distribution and mineral endowment. Precambrian Research 274 (2016) 61-81 http://dx.doi.org/10.1016/j.precamres.2015.05.028
30. McCuaig, T.C., Fougerouse, D., Salvi, S., Siebenaller, L., Parra-Avila, L. A., Seed, R., Béziat, D., & André-Mayer, A.S. (2016). The Inata deposit, Belahouro District, northern Burkina Faso. Ore Geology Reviews 78 (2016) 639–644. http://dx.doi.org/10.1016/j.oregeorev.2015.11.014
31. Mélisi, J.P., Ledru, P., Feybesse, J.L., Dammanget, A., & Marcoux, E. (1992). Early Proterozoic ore deposit and tectonics of the Birimian orogenic belt, West Africa. Precambrian Research 58, 305-344
32. Metelka, V., Baratoux, L., Naba, S., & Jessell, W.M. (2011). A geophysically constrained litho-structural analysis of the Eburnean greenstone belts and associated granitoid domains, western Burkina Faso. Precambrian Research. doi:10.1016/j.precamres.2011.08.002.
33. Murray, S., Torvela, T., & Bills, H. (2019). A geostatistical approach to analyzing gold distribution controlled by large-scale fault systems – An example from Cote d'Ivoire, Journal of African Earth Sciences 151 (2019) 351-370. https://doi.org/10.1016/j.jafrearsci.2018.12.019
34. Naba, S., Lompo, M., Débat, P., Bouchez, J.L., & Béziat, D. (2004). Structure and emplacement model for late-orogenic Paleoproterozoic granitoids: the Tenkodogo-Yamba elongate pluton (Eastern Burkina Faso). Journal of African Earth Sciences 38: 41–57.

 ISSN: 1857-7881 (Print) e - ISSN 1857-7431

35. Ouiya, P., Siebenaller, L., Salvi, S., Béziat, D., Naba, S., Baratoux, L., Naré, A., & Franceschi, G. (2015). The Nassara gold prospect, Gaoua District, southwestern Burkina Faso. Ore Geology Reviews (2015). http://dx.doi.org/10.1016/j.oregeorev.2015.11.026.
36. Passchier, C.W. & Rudolph, A.J.T. (2005). Microtectonic, 2nd, Revised and Enlarged edition. Springer. ISBN-10 3-540-64003-7 Springer Berlin Heidelberg New York
37. Pons, J., Barbey, P., Dupuis, D., & Léger, J. M. (1995). Mechanisms of pluton emplacement and structural evolution of a 2.1 Ga juvenile continental crust: the Birimian of southwestern Niger. Precambrian Research 70 (1995) 281-301.
38. Ramsay, J.G. (1967). Folding and fracturing of rocks. McGrmr-Hi//, inc., New York
39. Robert, F. (1990). Internal structure of the Cadillac Tectonic Zone southeast of Val d'Or, Abitibi Belt, Quebec. Canadian Journal of Earth Sciences 26 (12), 2661-2675, 1989.
40. Sawadogo, S., Naba, S., Ilboudo, H., Traoré, A.S., Nakolendoussé, S., & Lompo, M. (2018). The Belahourou granite pluton (Djibo greenstone belt, Burkina Faso): Emplacement mechanism and implication for gold mineralization along a shear zone. Journal of African Earth Sciences 148 (2018) 59-68. https://doi.org/10.1016/j.jafrearsci.2018.04.009.
41. Sawadogo, S., Yameogo, A.O., & Naba, S. (2021). Caractérisation des structures de déformation Éburnéennes dans la ceinture de roches vertes et les granitoïdes de la région de Zorgho (centre du burkinaFaso). Annales de l'Université Joseph KI-ZERBO – Série C, vol. 019, Décembre 2021 – ISSN : 2424 7545
42. Siagné, Z.H., Aïfa, T., Kouamelan, A.N., Houssou, N.N., Digbeu, W., Kakou, B.K.F., & Couderc, P. (2022). New lithostructural map of the Doropo region, northeast Ivory coast : Insight from structural and aeromagnetic data. Journal of African Earth Sciences 196 (2022) 104680.https://doi.org/10.1016/j.jafrearsci.2022.104680
43. Soumaila, A., Henry, P., & Rossy, M. (2004). Contexte de mise en place des roches basiques de la ceinture de roches vertes birimiennes de Diagourou-Darbani (Liptako, Niger, Afrique de l'Ouest) : Plateau océanique ou environnement d'arc/bassin arrière-arc océanique. Comptes Rendus Géosciences 336, 1137-1147
44. Sylvester, A.G. & Smith, R.R. (1976). Tectonic transpression and basement controlled deformation in San Andreas fault zone, Salton trough, California. American Association of Petroleum Geologists Bulletin; volume 60, page 2081-2102.

 ISSN: 1857-7881 (Print) e - ISSN 1857-7431

45. Tchalenko, J.S. & Ambrasey, N.N. (1970). Structural analysis of the Dasht-e Bayaz (Iran) earthquake fractures. Geological Society of America Bulletin; volume 81, pages 41-66.
46. Tshibubudze, A., Hein, K.A.A., & Marquis, P. (2009). The Markoye Shear Zone in northeast Burkina Faso. Journal of African Earth Sciences 55, 245-256.
47. Tshibubudze, A. & Hein, K.A.A. (2010). Tectonic evolution of the Oudalan-Gorouol greenstone belt in northeast Burkina Faso and Niger, West African craton. Geophysical research Abstracts 12, ECU2010-708 (2010 ECU General Assembly 2010, ISSN of eISSN: 1607-7962).
48. West African Resources LTD (n.d.). Toega Gold Project. https://www.westafricanresources.com/projects/sanbrado-project/
49. Woodman, K. K., Baratoux, L., Somda, A., & Siebenaller, L. (2015). The Youga gold deposit, Burkina Faso. Ore Geology Reviews (2015)